2007

Flow Boiling Heat Transfer in Microchannels

D. Liu

S V. Garimella
Purdue University, sureshg@purdue.edu

Liu, D. and Garimella, S V., "Flow Boiling Heat Transfer in Microchannels" (2007). *CTRC Research Publications.* Paper 264.
http://dx.doi.org/10.1115/1.2754944

Flow Boiling Heat Transfer in Microchannels

Dong Liu[1]
e-mail: dongliu@ecn.purdue.edu

Suresh V. Garimella
e-mail: sureshg@ecn.purdue.edu

Cooling Technologies Research Center,
School of Mechanical Engineering,
Purdue University,
West Lafayette, IN 47907-2088

Flow boiling heat transfer to water in microchannels is experimentally investigated. The dimensions of the microchannels considered are 275×636 *and* 406×1063 μm^2. *The experiments are conducted at inlet water temperatures in the range of* $67-95\,^{\circ}C$ *and mass fluxes of* $221-1283$ kg/m^2 s. *The maximum heat flux investigated in the tests is* 129 W/cm^2 *and the maximum exit quality is 0.2. Convective boiling heat transfer coefficients are measured and compared to predictions from existing correlations for larger channels. While an existing correlation was found to provide satisfactory prediction of the heat transfer coefficient in subcooled boiling in microchannels, saturated boiling was not well predicted by the correlations for macrochannels. A new superposition model is developed to correlate the heat transfer data in the saturated boiling regime in microchannel flows. In this model, specific features of flow boiling in microchannels are incorporated while deriving analytical solutions for the convection enhancement factor and nucleate boiling suppression factor. Good agreement with the experimental measurements indicates that this model is suitable for use in analyzing boiling heat transfer in microchannel flows.* [DOI: 10.1115/1.2754944]

Keywords: microchannels, boiling, high heat flux, heat sink

1 Introduction

Boiling heat transfer in microchannel heat sinks has attracted significant interest due to its capability for dissipating the high heat fluxes encountered in the thermal management of microelectronics [1,2]. However, the complex nature of convective flow boiling and two-phase flow in microchannels is still not well understood and has impeded the practical implementation of microchannel heat sinks with two-phase flow [3–5]. Among the unresolved issues of particular importance is the quantitative prediction of the boiling heat transfer coefficient in microchannels over a wide range of conditions, from subcooled to saturated boiling. A limited number of studies in the literature [6–17] have addressed this issue, as summarized in Table 1. A survey of this literature reveals a lack of consensus on the understanding and prediction of boiling heat transfer and two-phase flow in microchannels. In particular, although flow-pattern-based models [18,19] have been proposed to correlate boiling data, these models are typically applicable over a narrow range of experimental conditions. There is thus a clear need for additional systematic studies, which carefully address the experimental characterization and modeling of boiling heat transfer in microchannel flows.

The objective of the present work is to conduct a comprehensive experimental investigation of flow boiling heat transfer in microchannel heat sinks, covering a range of subcooled and saturated boiling conditions. The subcooled and saturated boiling regimes are studied in the lower quality range (up to 20%). Heat flux, temperature, and pressure drop measurements are used to construct boiling curves. Boiling heat transfer correlations developed for conventional-sized channels are critically appraised for their applicability to the prediction of flow boiling in microchannels. A heat transfer correlation suitable for prediction of heat transfer coefficients in the subcooled boiling regime is identified. A new superposition model is developed as a modification to the model of Chen and co-workers [20,21] to correlate the results in the saturated boiling regime; the proposed model incorporates the unique flow features of microchannel flows. The model predictions are validated against the experimental results.

2 Experiments

2.1 Experimental Setup. Figure 1(*a*) shows the test loop assembled for the experimental investigation of convective flow boiling in microchannels. A variable-speed gear pump is used to circulate the working fluid (de-ionized water) through the test loop. Two turbine flowmeters are arranged in parallel to measure flow rates in different ranges during the tests. A water bath adjusts the degree of subcooling in the fluid prior to entering the microchannel heat sink. A liquid-to-air heat exchanger is employed to condense the vapor in the two-phase mixture before the fluid returns to the reservoir. The absolute pressures in the entrance and exit manifolds of the microchannel test section are measured. The experimental data are read into a data acquisition system for processing.

The microchannel test section consists of a copper test block, an insulating G10 housing piece, and a G7 fiberglass cover, as shown in Figs. 1(*b*) and 1(*c*). Twenty-five microchannels were cut into the top surface of the copper block, which has an area of 25.4×25.4 mm^2 using a precision sawing technique. Test pieces with two different microchannel dimensions were tested. The first test piece (microchannel I) contains microchannels that are 275 μm in width (w_c) and 636 μm in height (H_c), with an intervening fin thickness (w_w) of 542 μm, while the second test piece (microchannel II) contains microchannels that are 406 μm in width and 1063 μm in height, with an intervening fin thickness of 597 μm. Eight cartridge heaters embedded in the copper block provide a maximum power input of 1600 W. As indicated in Fig. 1(*c*), three Copper-Constantan (type-T) thermocouples (T_1-T_3) made from 36-gauge wire were inserted just below the microchannels at a distance of 3.17 mm from the base. Microchannel wall temperatures at the three streamwise locations are obtained by extrapolation from these three thermocouple readings. Four more thermocouples (T_1-T_3) were embedded in the copper block at 6.35 mm axial intervals for measurement of the average heat flux. The inlet and outlet fluid temperatures ($T_{f,\mathrm{in}}$ and $T_{f,\mathrm{out}}$) were measured at locations immediately upstream and downstream of the

[1]Corresponding author.

Contributed by the Heat Transfer Division of ASME for publication in the JOURNAL OF HEAT TRANSFER. Manuscript received August 21, 2006; final manuscript received December 14, 2006. Review conducted by Satish G. Kandlikar. Paper presented at the 2005 ASME International Engineering Congress (IMECE2005), Orlando, FL, November 5–11, 2005.

Table 1 Studies of flow boiling in microchannels in the literature

Reference	Dimension	Fluid	Parameter range	Key observations	Heat transfer correlation
Lazarek and Black [6]	D_h=3.15 mm	R-113	G: 140–740 kg/s m^2	Heat transfer coefficient relatively independent of vapor quality, and function of Nu, Re, and Bo	$\mathrm{Nu}=30\,\mathrm{Re}^{0.857}\,\mathrm{Bo}^{0.714}$
			x: 0–0.8	Nucleate boiling dominates	
Wambsganss et al. [7]	D_h=2.92 mm	R-113	G: 50–300 kg/s m^2	Nucleate boiling dominates	
			x: 0–0.9	Heat transfer coefficient strongly dependent on heat flux and weakly dependent on mass flux and quality	
Tran et al. [8]	D_h=2.4 mm	R-12	G: 44–832 kg/s m^2	Nucleate boiling dominates	$\mathrm{Nu}=770(\mathrm{Re}_{Lo}\,\mathrm{Co}\,\mathrm{Bo})^{0.62}\left(\frac{\rho_g}{\rho_l}\right)^{0.297}$
			x: 0–0.94	Heat transfer coefficient independent of quality for $x>0.2$ and has no mass flux dependence	
Kew and Cornwell [9]	D_h=1.39–3.69 mm	R-141b		Heat transfer coefficient shows different trends for high and low mass flux	
Yan and Lin [10]	D_h=2 mm	R-134a	G: 50–200 kg/s m^2	Variation of heat transfer coefficient with quality is not consistent and depends on heat flux, saturation temperature, and mass flux	$h_{\mathrm{tp}}=(C_1\mathrm{Co}^{C_2}+C_3\mathrm{Bo}^{C_4}\,\mathrm{Fr}_{lo})(1-X_m)^{0.8}h_l$
			x: 0–0.9		
Bao et al. [11]	D_h=1.95 mm	R11 HCFC123	G: 50–1800 kg/s m^2	Nucleate boiling dominates	$h=C_1 q''^{C_2}$
			x: 0–0.9	Heat transfer coefficient independent of mass flux and vapor quality and increases with heat flux and system pressure for saturated regime	
Lee and Lee [12]	20×0.4–2 mm	R-113	G: 50–200 kg/s m^2	Heat transfer dominated by convection	Film-flow model applicable for low flow rate; Kandlikar correlation applicable for high flow rate
			x: 0.15–0.75	Heat transfer coefficient independent of heat flux and increases with mass flux and vapor quality.	
Yu et al. [13]	D_h=2.98 mm	Water	G: 50–200 kg/s m^2	Nucleate boiling dominates over a large mass flux and quality range	$h=6{,}400{,}000(\mathrm{Bo}\,\mathrm{We})^{0.27}\left(\frac{\rho_l}{\rho_v}\right)^{-0.2}$
			x: 0–0.9		
Qu and Mudawar [14]	231×713 μm^2	Water	G: 134–402 kg/s m^2	Forced convection heat transfer dominant in saturated boiling	Annular model proposed
			x: 0–0.2		
Haynes and Fletcher [15]	D_h=0.92 mm	R11	G: 110–1840 kg/s m^2	Nucleate boiling dominates as subcooled liquid approaches saturation	$h=h_{\mathrm{conv}}+h_{\mathrm{pb}}(q_{\mathrm{nb}})\frac{T_w-T_{\mathrm{sat}}}{T_w-T_{\mathrm{mean}}}$
	1.95 mm	HCFC123	x: −0.35–1.0	No suppression of nucleate boiling if $\mathrm{Re}_{\mathrm{LO}}<10^4$ h_{conv} for larger than single-phase value, strongly correlated with nucleate boiling	
Warrier et al. [16]	D_h=0.75 mm	FC-84	G: 557–1600 kg/s m^2	No significant maldistribution for five-channel configuration	Subcooled region
					$\frac{h_{\mathrm{tp}}}{h_{\mathrm{sp\_FD}}}=1+6.0\mathrm{Bo}^{1/16}+290(1-855\mathrm{Bo})\mathrm{Sc}^{4.15}$
			x: 0–0.2	Flow pattern develops quickly into annular flow	Saturated region
					$\frac{h_{\mathrm{tp}}}{h_{\mathrm{sp\_FD}}}=1+6.0\mathrm{Bo}^{1/16}-5.3(1-855\mathrm{Bo})X^{0.65}$
Chen and Garimella [17]	504×2500 μm^2	FC-77		Nucleate boiling heat transfer dominant	

microchannels, respectively. The power input to the cartridge heaters was regulated by a digitally controlled dc power supply unit.

2.2 Test Procedure. Prior to each experiment, the working fluid was degassed by violently boiling the water for approximately 1 h. The amount of dissolved gas in the water was monitored with an in-line oxygen sensor and the water was considered degassed when the concentration was less than 4 ppm; at this concentration, the effects of dissolved gas on the boiling heat transfer may be neglected [22].

In each experiment, the heater power supply was switched on and set to the desired value after the fluid inlet temperature was stabilized. A steady state was reached when readings from all thermocouples remained unchanged (within ±0.1 °C) over a 2 min period. Each steady-state value was calculated as an average of 300 readings for all power, temperature, pressure, and flow rate measurements. The heat flux was then increased for the next test, and the procedure repeated for subsequent tests. The fluid inlet velocity and temperature were varied to achieve different testing conditions, as summarized for both microchannel dimensions in Tables 2 and 3. The maximum heat flux in the experiments was 128.8 W/cm^2. The inlet temperature of water is adjusted as a parameter, and varies between 66.6 and 94.9 °C for microchannel I and 78.8 and 95.4 °C for microchannel II. If the fluid were introduced at near-saturated conditions, the distribution of the two-phase mixture in the microchannels would be heavily affected by the entrance manifold, with the flow boiling patterns in the microchannels being a function of the particular entrance conditions used.

2.3 Data Reduction. The heat loss to the ambient from the test section is estimated from the difference between the total power input q_{input} and the sensible heat gain by the fluid under single-phase heat transfer conditions as

$$q_{\mathrm{loss}}=q_{\mathrm{input}}-\dot{m}c_p(T_{f,\mathrm{out}}-T_{f,\mathrm{in}}) \tag{1}$$

and is correlated as a function of the average wall temperature $q_{\mathrm{loss}}=q_{\mathrm{loss}}(T_{w,m})$ for each inlet condition, which is then used in calculating heat loss under boiling conditions. Once boiling commences, between 87% and 98% of the input power was transferred to the water under the range of experimental conditions considered, depending on the heat flux and flow rate.

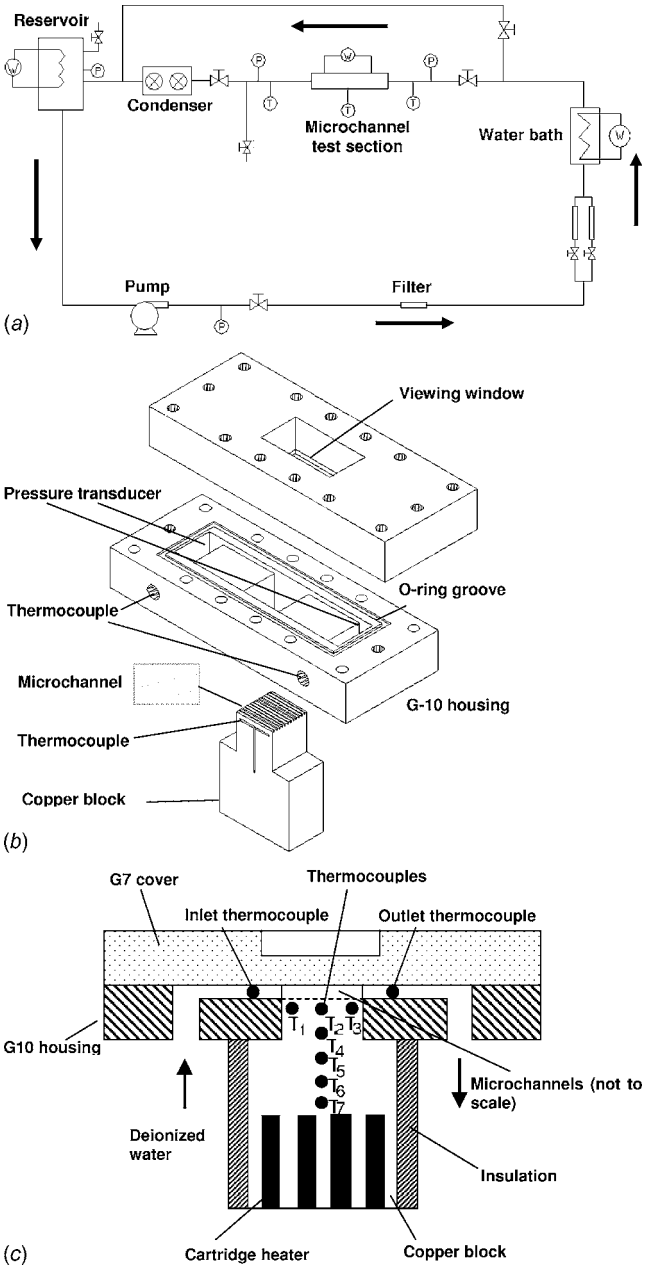

Fig. 1 Experimental setup for studying flow boiling in a microchannel heat sink: (*a*) test loop, (*b*) test piece assembly, and (*c*) cross-sectional view of the microchannel test piece

The applied heat flux q'' is calculated using the base area of the copper block, $A_b = WL$, and represents the heat dissipation rate of the heat sink,

$$q'' = (q_{\text{input}} - q_{\text{loss}})/A_b \tag{2}$$

The effective wall heat flux is defined as

$$q''_w = (q_{\text{input}} - q_{\text{loss}})/A_t \tag{3}$$

where A_t $(=n(w_c + 2\eta H_c L))$ is the total heat transfer area of the microchannels.

The microchannel length can be divided into two regions according to the local thermodynamic quality:

Table 2 Test matrix for microchannel flow boiling experiments: microchannel I

Case	u_0 (m/s)	G (kg/s m^2)	$T_{f,\text{in}}$ (°C)	$q''_{\max}$ (W/cm^2)	$x_{\text{exit,max}}$
I-1	0.33	324	66.6	111.1	0.16
I-2	0.34	327	77.9	116.1	0.19
I-3	0.33	319	78.7	106.5	0.18
I-4	0.33	323	84.8	119.7	0.20
I-5	0.33	322	89.2	115.4	0.20
I-6	0.33	321	94.9	106.1	0.19
I-7	0.68	663	66.5	117.8	0.05
I-8	0.67	651	77.6	99.1	0.05
I-9	0.68	655	85.7	111.2	0.07
I-10	0.68	661	89.2	118.0	0.08
I-11	0.68	662	78.9	112.7	0.06
I-12	0.68	652	94.8	96.4	0.07
I-13	0.95	921	78.3	104.3	0.03
I-14	0.95	919	85.6	117.1	0.05
I-15	0.96	926	93.2	115.1	0.06
I-16	1.33	1283	87.8	114.7	0.03

$$x = \frac{i_f - i_{\text{sat},0}}{h_{\text{fg}}} \tag{4}$$

The subcooled region covers the portion of the channel over which the thermodynamic quality takes negative values. In terms of flow regimes, it includes both the single-phase and subcooled boiling regions. The length of the subcooled region can be calculated from the following energy balance:

$$L_{\text{sp}} + L_{\text{sub}} = \frac{\dot{m}c_p(T_{\text{sat},0} - T_{f,\text{in}})}{q''W} \tag{5}$$

in which $T_{\text{sat},0}$ is the local saturation temperature, and L_{sp} and L_{sub} are the lengths of the single-phase and subcooled boiling regions, respectively. In the saturated region that follows, the temperature of the vapor-liquid mixture remains at the local saturation point and the quality increases from zero as the fluid picks up more heat, adding to the vapor content of the flow.

The boiling heat transfer coefficient is determined from

$$\bar{h}_{\text{tp}} = \frac{q''_w}{T_w - T_f} \tag{6}$$

in which T_w is the average temperature of the channel wall and T_f is the mean fluid temperature.

Temperature-dependent thermophysical properties of water were used for both the liquid and vapor phases in the data analysis. The saturation temperatures at the inlet and outlet were determined from the pressure measurements. Then, following the ap-

Table 3 Test matrix for microchannel flow boiling experiments: microchannel II

Case	u_0 (m/s)	G (kg/s m^2)	$T_{f,\text{in}}$ (°C)	$q''_{\max}$ (W/cm^2)	$x_{\text{exit,max}}$
II-1	0.23	224	79.7	120.9	0.093
II-2	0.23	221	91.7	116.9	0.112
II-3	0.23	224	94.5	122.2	0.116
II-4	0.25	241	94.8	126	0.113
II-5	0.31	299	80.8	121.4	0.062
II-6	0.31	299	85.9	117.3	0.067
II-7	0.31	297	91.9	121.9	0.082
II-8	0.31	297	94.7	108.6	0.07
II-9	0.34	332	78.8	118.3	0.049
II-10	0.34	330	92.1	112.5	0.06
II-11	0.34	328	95.1	118.9	0.069
II-12	0.37	360	79.8	120.2	0.044
II-13	0.37	361	91.8	128.8	0.068
II-14	0.37	357	94.5	114.9	0.059
II-15	0.37	357	95.4	125.4	0.067

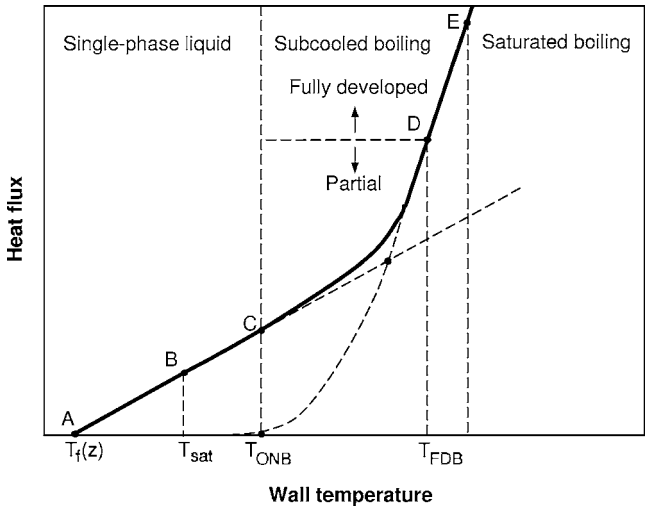

Fig. 2 Boiling curve: variation of wall temperature and heat flux during flow boiling in channels

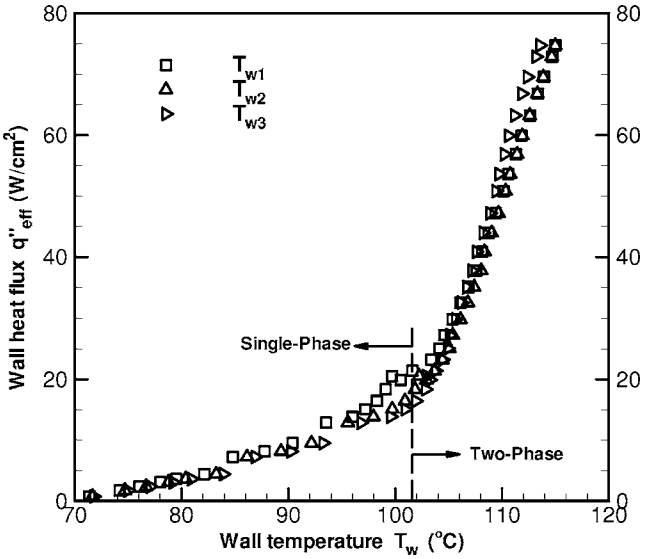

Fig. 3 Boiling curve, case I-1 (G=324 kg/m^2 s, $T_{f,in}$=66.6°C)

proach of Collier [23], a linear profile is assumed for the local saturation temperature between the inlet and outlet, and the local saturation temperature $T_{sat,0}$ in Eq. (5) is obtained as its intersection point with the single-phase temperature curve.

2.4 Measurement Uncertainties. The uncertainty in temperature measurements was estimated to be ±0.3°C with the T-type thermocouples employed. The flowmeter was calibrated with a weighing method, yielding a maximum uncertainty of 2.4%. The measurement error for the pressure transducer was 0.25% of full scale (1 atm). Uncertainty associated with the heat flux measurement was in the range of 3.1–7.5%. A standard error analysis [24] revealed uncertainties in the reported heat transfer coefficient to be in the range of 5–9.4%. Experiments conducted over a period of months showed good repeatability.

3 Experimental Results

Experimental measurements of wall temperature and pressure drop are presented in this section to characterize the boiling heat transfer features in the microchannel flows tested.

The boiling curve shown in Fig. 2 schematically illustrates the wall temperature variation as a function of heat flux. The fluid enters the channel at point A as subcooled single-phase liquid. The heat transfer mode is single-phase convective heat transfer until location C, at which point the wall temperature exceeds the threshold value for the onset of nucleate boiling (ONB). From this point onward, both single-phase convection and nucleate boiling contribute to the total heat transfer. The convective component is then swamped by boiling heat transfer from point D when the fully developed boiling region (FDB) starts. The intermediate region (C–D) is defined as the partial boiling regime. As fluid continues to absorb heat, saturated boiling is established at location E, when the bulk temperature reaches the local saturation temperature. Beyond this point, the vapor content increases steadily until dryout occurs. In the present work, the subcooled and the saturated boiling regimes are studied.

Figure 3 shows representative boiling curves measured in the experiments at the three streamwise locations for case I-1 (details as in Table 2). The ONB can be clearly identified in the figure as the point where the wall temperature exhibits a change in slope from the single-phase dependence. In the two-phase regime, the rise in wall temperature over a wide range of wall heat flux is modest as expected. At a sufficiently high heat flux in the two-phase regime, the wall temperature near the channel exit (T_3) drops below that at the upstream locations. This is caused in part by the reduction in local saturation temperature of water when saturated boiling occurs.

The effects of inlet fluid temperature and velocity on the boiling curves are shown in Figs. 4 and 5. The wall temperatures shown in these figures are those measured near the exit of the microchannel, i.e., from thermocouple T_{w3}. It is observed that in the single-phase region the fluid with lower inlet temperature or velocity is able to dissipate higher heat fluxes while maintaining the same wall superheat. However, after the ONB, all boiling curves collapse onto a single curve irrespective of the inlet conditions, indicating the dominance of nucleate boiling over convective heat transfer.

The measured pressure drop across the microchannel heat sink as the flow transitions from single-phase to two-phase operation is shown in Fig. 6; the pressure drop is measured between the two manifolds upstream and downstream and inlet/exit losses are corrected for as recommended in Ref. [25]. In the single-phase region, the pressure drop slightly decreases as the heat flux in-

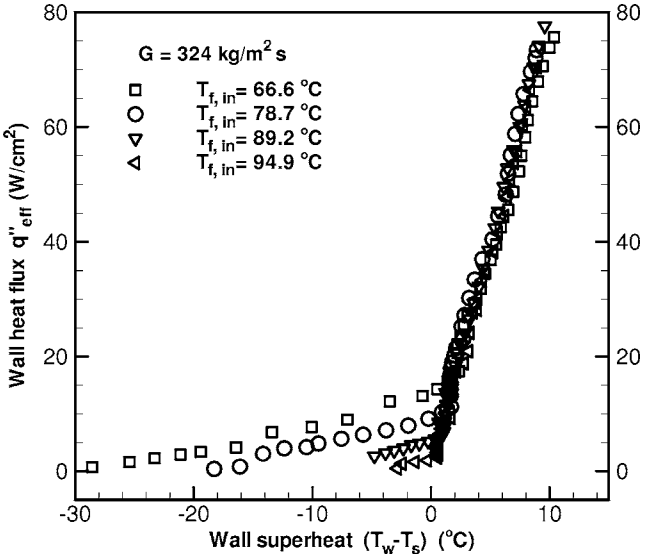

Fig. 4 Effect of inlet temperature on the boiling curves (wall temperature measured for microchannel I at $T_{w,3}$)

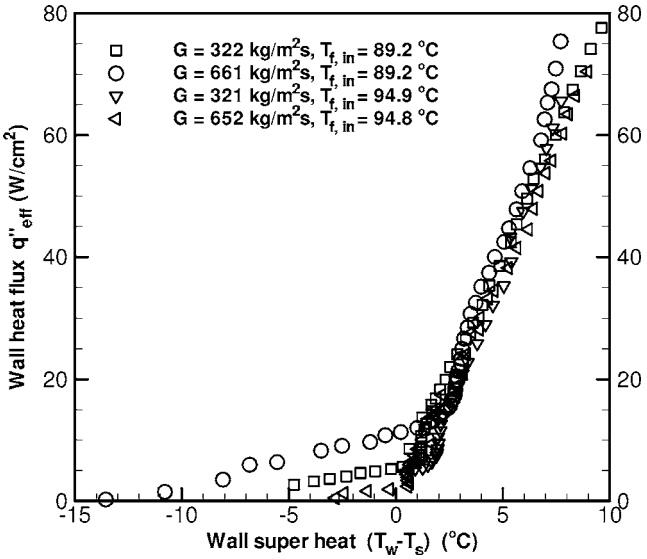

Fig. 5 Effect of inlet velocity on boiling curves (wall temperature measured for microchannel I)

creases due to the reduced viscosity of water at higher temperatures. After the ONB, the pressure drop increases rapidly when the acceleration effect of the vapor content becomes pronounced. It may be noted that both Figs. 3 and 6 provide consistent predictions of the incipience heat flux for the ONB, i.e., at $q''=15\ \mathrm{W/cm^2}$.

The experimental results are discussed further after a presentation of the development of predictive models for flow boiling heat transfer.

4 Modeling of the Flow Boiling Heat Transfer Coefficient

Flow boiling heat transfer is strongly influenced by the morphological structure of the liquid-vapor mixture, i.e., the flow pattern [26]. Flow-pattern-based models are thus capable of providing more accurate predictions of local boiling heat transfer coefficient [18,19]. However, the purpose of the present study is to offer easy-to-use predictive tools that capture the global heat transfer behavior and can be applied to the design of two-phase microchannel heat sinks. Therefore, a correlation-based approach is adopted in this study for modeling the flow boiling heat transfer coefficient. Detailed flow-pattern-based modeling of bubbly, slug, and annular flows is the subject of ongoing work.

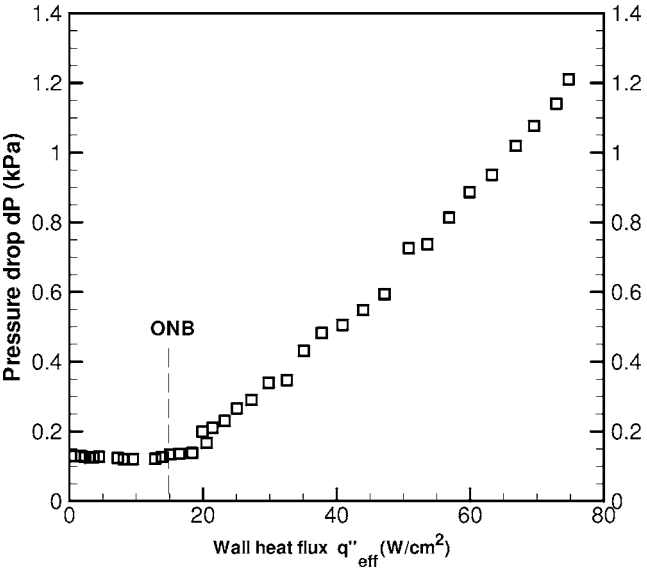

Fig. 6 Pressure drop, case I-1 (G=324 kg/m² s, $T_{f,\mathrm{in}}$=66.6°C)

Correlation-based models for the flow boiling heat transfer coefficient, in both subcooled and saturated boiling, have been classified into two categories [27,28]: the extrapolation type (termed "enhancement type" in Ref. [28]) and the superposition type (further divided into superposition and asymptotic types in Ref. [28]). The first of these involves extrapolating single-phase convection data into the boiling regime by correlating the heat transfer coefficient as a function of the boiling number (Bo) and the convection number (Co), and relying on experimental databases (subcooled boiling [27,29–32] and saturated boiling [6,8,13,33–35]). This approach is expected to work reasonably well in the subcooled boiling regime, where heat transfer is primarily due to singe-phase convection and a modification factor using dimensionless groups is adequate for representing the enhancement due to nucleate boiling. However, when applied beyond regions for which they were proposed, the extrapolation approach is of limited value. Further, the functional form of the nondimensional groups involved may not adequately represent the most important parameters of the boiling process. In contrast, the second approach, superposition, deals with both single-phase and nucleate boiling heat transfer modes that are present in the two-phase flows, and treats the total heat transfer as either a linear or a power-type superposition of single-phase convection and nucleate boiling components (subcooled boiling [36–38] and saturated boiling [20,21,36,37,39]). This approach is more physically sound and may be tailored to different flow and heat transfer situations, such as laminar versus turbulent flows. A superposition-type approach is, therefore, used in this work for the development of a model for saturated boiling.

In the following, boiling regimes are first analyzed to set the context for assessing the applicability of selected heat transfer correlations in predicting boiling heat transfer in microchannel flow. It will be shown that Shah's correlation [38] from the literature is suitable for the subcooled boiling regime, and therefore, the emphasis here is placed on developing a new model for the saturated boiling regime as a modification to an earlier model [20], which incorporates some of the specific features of flow boiling in microchannels.

4.1 Models for Different Heat Transfer Regions. Under commonly encountered flow conditions, the fluid enters the microchannel with some degree of subcooling and exits as a saturated liquid-vapor mixture. Thus, three regions—single-phase flow, subcooled boiling, and saturated boiling—can exist along the microchannel length. The single-phase length L_{sp} can be calculated from Eq. (5), which, combined with the ONB model developed in Ref. [40],

$$\sqrt{T_{f,\mathrm{in}}+\frac{q''Wz_{\mathrm{ONB}}}{\rho_f c_p u_0 (nw_c H_c)}+\frac{\{[\alpha/(1+2\eta\alpha)][(w_c+w_w)/H_c]\}q''}{(Nu_z k_f)/D_h}}-\sqrt{T_s}=\sqrt{\frac{2\sigma C}{\rho_v h_{fg}}\frac{\{[\alpha/(1+2\eta\alpha)][(w_c+w_w)/H_c]\}q''}{k_f}} \tag{7}$$

yields the subcooled boiling length L_{sub}. Figure 7 illustrates the variation of length ratio of the different boiling regions as the heat input changes. At very low heat input, the fluid in the entire microchannel remains a single-phase liquid, shown as region I. As the heat input increases, nucleate boiling occurs first at the exit of the microchannel and then shifts upstream. The shift of the boiling front is very rapid, and with a slight increase in heat input, the subcooled boiling regime occupies an appreciable portion of the microchannel length, as indicated by region II. Further increasing the heat input results in saturated boiling in the microchannel (as

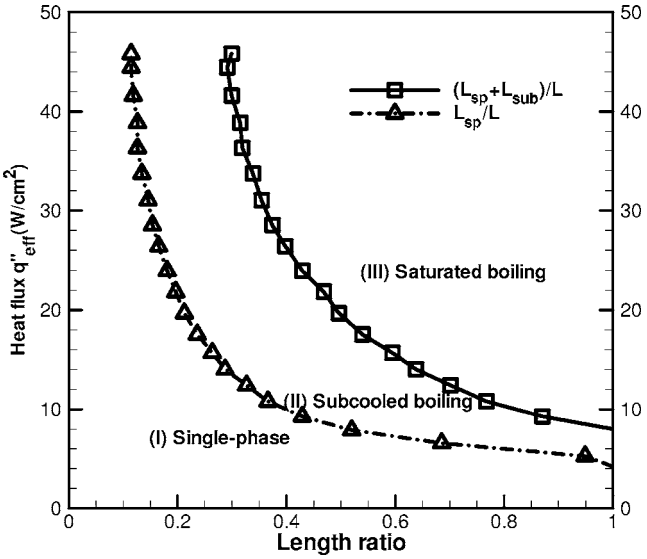

Fig. 7 Three boiling regimes in a microchannel, case II-10 (G = 330 kg/m² s, $T_{f,\text{in}}$ = 92.1 °C)

shown in region III).

In view of the existence of the three heat transfer regions, it is reasonable to define the average boiling heat transfer as

$$\bar{h} = (h_{\text{sp}}L_{\text{sp}} + h_{\text{sub}}L_{\text{sub}} + h_{\text{sat}}L_{\text{sat}})/L \tag{8}$$

This definition describes the overall heat transfer in microchannel flows, independent of specific flow patterns. It now remains to obtain the heat transfer coefficients for the respective regions in Eq. (8) as follows.

Single-Phase Regime. The selection of the correlation for predicting single-phase heat transfer plays an important role in the success of any proposed equation for analyzing flow boiling. The Dittus-Boelter correlation for turbulent flow [41] has been widely adopted for this purpose [20,30,34,38]. However, its applicability to microchannel transport is questionable since laminar flow is typically encountered in microchannels ($\text{Re}_f < 1600$ in the present work). Thus, laminar correlations should be employed instead, for instance, the Sieder–Tate correlation [42] for simultaneously developing flow or the Shah–London correlation [43] for thermally developing flow, depending on the thermal and hydrodynamic boundary conditions. Lee et al. [44] pointed out that a full computational heat transfer analysis is necessary for an accurate description of the heat transfer in microchannels. However, the foregoing equations are reasonable approximations, which are useful for correlating the boiling data due to their simple functional forms.

Subcooled Boiling Regime. Among the subcooled boiling heat transfer correlations in the literature, the one proposed by Shah [38] is among the more often cited:

$$h_{\text{tp}} = h_{\text{sp}}\left[1 + (\psi_0 - 1)\frac{T_w - T_s}{T_w - T_f}\right] \tag{9}$$

In Eq. (9), ψ_0 is the contribution from the limiting case of subcooled cooling, i.e., saturated boiling with zero subcooling and zero quality. The following expressions have been suggested in Ref. [38] for this term:

$$\psi_0 = \begin{cases} 230\text{Bo}^{0.5} & (\text{Bo} > 3 \times 10^{-5}) \\ 1 + 46\text{Bo}^{0.5} & (\text{Bo} < 3 \times 10^{-5}) \end{cases} \tag{10}$$

It will be shown that predictions from this correlation show good agreement with the experimental measurements for microchannels in the present work. Two other commonly cited correlations, due to Moles–Shaw [27] and Kandlikar [32], are also considered in the comparisons with the experimental results in Sec. 5.

Saturated Boiling Regime. In superposition-type models, starting from that of Rohsenow [45], it is postulated that convective heat transfer is promoted as the flow is agitated by bubble nucleation and growth, while nucleate boiling is suppressed owing to the reduced superheat in the near-wall region caused by the bulk fluid flow. The simplest form of the superposition approach uses a linear addition as in the model of Chen and co-workers [20,21,46]:

$$h_{\text{tp}} = h_{\text{conv}} + h_{\text{boiling}} = Fh_{\text{sp}} + Sh_{\text{nb}} \tag{11}$$

in which the enhancement factor F for convection and the suppression factor S for nucleate boiling are given by

$$F = \phi_{f,\text{tt}}^{0.89} = (1 + X_{\text{tt}}^{-0.5})^{1.78} \tag{12}$$

$$S = 0.9622 - 0.5822\left[\tan^{-1}\left(\frac{\text{Re}_f F^{1.25}}{6.18 \times 10^4}\right)\right] \tag{13}$$

and $\phi_{f,\text{tt}}$ is the two-phase multiplier for turbulent-turbulent flows and X_{tt} is the corresponding Martinelli parameter. In Ref. [20], the single-phase heat transfer coefficient was represented by the Dittus–Boelter correlation for turbulent flow, and the Forster–Zuber correlation [47] was used to estimate the nucleate boiling heat transfer coefficient.

More recently, a modification of the model of Chen and coworkers has been proposed for flow boiling in microchannels [48,49]. Two alternative approaches were suggested to amend the enhancement factor F for microchannel flows. The first approach [48] is essentially a curve-fitting technique that forces the enhancement factor F to be linearly related to the two-phase friction multiplier, i.e., $F = 0.64\phi_{f,\text{tt}}$, in contrast to Eq. (12). This functional form is then generalized to the two-phase multipliers for other flow conditions, including the laminar-laminar flow in microchannels. In the second approach [49], a boiling heat transfer coefficient was derived for annular flow and used as the convective component h_{conv} in Eq. (11); however, such a substitution does not derive from the flow physics and is somewhat arbitrary. Although predictions from this model showed reasonable agreement with the experimental data the authors compiled from different studies in the literature, a more physically sound model is desired to capture the important features of flow boiling in microchannels.

4.2 New Model Development for Saturated Boiling. The superposition-type approach above is modified here to account for the specific features of flow through microchannels. New correlations for the enhancement factor F and suppression factor S are derived following Chen [20] and Bennett et al. [50].

Enhancement Factor F. It is assumed that the convective component in Eq. (11) can still be written in the form of the Sieder–Tate correlation [42] even in two-phase flow:

$$h_{\text{conv}} = 1.86(\text{Re}_{\text{tp}}\text{Pr}_{\text{tp}}D_h/L)^{1/3}\left(\frac{\mu_{\text{tp}}}{\mu_w}\right)^{0.14}\left(\frac{k_{\text{tp}}}{D_h}\right) \tag{14}$$

Here, the two-phase Reynolds number Re_{tp} is an unknown and is introduced in order to retain the functional form of Eq. (14):

$$\text{Re}_{\text{tp}} = \frac{\rho_f V_{\text{tp}} D_h}{\mu_f} \tag{15}$$

in which V_{tp} is a nominal two-phase velocity. Comparing Eq. (14) with the original Sieder–Tate correlation leads to

$$h_{\text{conv}} = h_{\text{sp}}\left(\frac{\text{Re}_{\text{tp}}}{\text{Re}_f}\right)^{1/3}\left(\frac{\mu_{\text{tp}}}{\mu_f}\right)^{0.14}\left(\frac{k_{\text{tp}}}{k_f}\right) \tag{16}$$

where the liquid Reynolds number Re_f is based on the liquid velocity V_f, for only liquid flowing in the channel, and is given by

$$\text{Re}_f = \frac{G(1-x)D_h}{\mu_f} = \frac{\rho_f V_f D_h}{\mu_f} \tag{17}$$

The enhancement factor F can then be obtained as

$$F = \frac{h_{\text{conv}}}{h_{\text{sp}}} = \left(\frac{\text{Re}_{\text{tp}}}{\text{Re}_f}\right)^{1/3}\left(\frac{\mu_{\text{tp}}}{\mu_f}\right)^{0.14}\left(\frac{k_{\text{tp}}}{k_f}\right)\left(\frac{\text{Pr}_{\text{tp}}}{\text{Pr}_f}\right)^{1/3} \tag{18}$$

Following Reynolds analogy, if it is assumed that the shear stress and heat flux profiles are similar, so that

$$\frac{q''(y)}{q''_w|_{y=0}} = \frac{\tau(y)}{\tau_w|_{y=0}} = f(y) \tag{19}$$

Using the definitions of shear stress and heat flux, Eq. (19) can be rearranged as

$$q''_w|_{y=0}du = -\frac{k}{\mu}\tau_w|_{y=0}dT \tag{20}$$

Assuming that the nominal velocity V_{tp} corresponds to the velocity at a distance from the wall where the local temperature T reaches the bulk mean value T_b, Eq. (20) can be integrated as

$$\int_0^{V_{\text{tp}}} q''_w du = -\int_{T_w}^{T_b} \frac{k}{\mu}\tau_w dT \tag{21}$$

which yields

$$q''_w V_{\text{tp}} = \frac{k}{\mu}\tau_w(T_w - T_b) \tag{22}$$

Recalling the definition of boiling heat transfer coefficient, the following expression is obtained:

$$h_{\text{conv}} = \frac{q''_w}{T_w - T_b} = \frac{k}{\mu}\frac{\tau_w}{V_{\text{tp}}} = \frac{\tau_w c_p}{\text{Pr}_{\text{tp}} V_{\text{tp}}} \tag{23}$$

For the liquid phase flowing alone in the channel, a similar expression can be derived

$$h_{\text{sp}} = \frac{\tau_{w,f} c_{p,f}}{\text{Pr}_f V_f} \tag{24}$$

Therefore, the ratio of boiling convection to single-phase convection defines the enhancement factor F:

$$\frac{h_{\text{conv}}}{h_{\text{sp}}} = \left(\frac{\tau_{w,\text{tp}}}{\tau_{w,f}}\right)\left(\frac{\text{Re}_f}{\text{Re}_{\text{tp}}}\right)\left(\frac{c_{p,\text{tp}}}{c_{p,f}}\right)\left(\frac{\text{Pr}_f}{\text{Pr}_{\text{tp}}}\right) = F \tag{25}$$

Combining with Eq. (18) and solving for $(\text{Re}_{\text{tp}}/\text{Re}_f)$ yield

$$\left(\frac{\text{Re}_{\text{tp}}}{\text{Re}_f}\right) = \left[\left(\frac{\tau_{w,\text{tp}}}{\tau_{w,\text{sp}}}\right)\left(\frac{\mu_f}{\mu_{\text{tp}}}\right)^{0.14}\left(\frac{k_f}{k_{\text{tp}}}\right)\left(\frac{\text{Pr}_f}{\text{Pr}_{\text{tp}}}\right)^{4/3}\left(\frac{c_{p,\text{tp}}}{c_{p,f}}\right)\right]^{3/4} \tag{26}$$

In Eq. (26), the shear stress term is linked to the two-phase multiplier ϕ_f as

$$\frac{\tau_{w,\text{tp}}}{\tau_{w,f}} = \frac{[(dp/dz)F]_{\text{tp}}}{[(dp/dz)F]_f} = \phi_f^2 \tag{27}$$

The expression for enhancement factor F is then obtained as

$$F = (\phi_f^2)^{1/4}\left(\frac{\mu_{\text{tp}}}{\mu_f}\right)^{0.105}\left(\frac{c_{p,\text{tp}}}{c_{p,f}}\right)^{1/4}\left(\frac{k_{\text{tp}}}{k_f}\right)^{3/4} \tag{28}$$

To account for the asymptotic behavior of two-phase convective heat transfer at the beginning of saturated flow boiling, an adjustable parameter ζ is now introduced. In the present study, ζ takes a value of 2, which gives a better fit to the experimental data than the value of 0.64 used in Ref. [49]. The reason for not choosing a value of unity for ζ (which would imply that F reduces to unity at zero quality and the convection contribution is simply represented by the single-phase component) is that the interactions between the bubble and fluid occur well before the flow reaches saturated boiling and the agitation of the fluid due to the bubble dynamics enhances convection even prior to reaching saturation. In addition, the use of a correction factor $\text{Pr}_f^{0.167}$ was suggested by Benett and Chen [46] when applying the Reynolds analogy to fluids with Prandtl number not equal to unity. The final form of enhancement factor F is

$$F = \zeta(\phi_f^2)^{1/4}\left(\frac{\mu_{\text{tp}}}{\mu_f}\right)^{0.105}\left(\frac{c_{p,\text{tp}}}{c_{p,f}}\right)^{1/4}\left(\frac{k_{\text{tp}}}{k_f}\right)^{3/4}\text{Pr}_f^{0.167} \tag{29}$$

The two-phase multiplier can be related to the Martinelli parameter as [51]

$$\phi_f^2 = 1 + \frac{C}{X} + \frac{1}{X^2} \tag{30}$$

in which the constant C is determined from Ref. [51] and Table 4, depending on the flow regimes of the liquid and vapor phases in microchannels. For the laminar flows (in both liquid and vapor phases) present in this study, the Martinelli parameter is

$$X^2 = \frac{[(dp/dz)F]_f}{[(dp/dz)F]_v} = \left(\frac{1-x}{x}\right)\left(\frac{\rho_v}{\rho_f}\right)\left(\frac{\mu_f}{\mu_v}\right) \tag{31}$$

Thus, Eqs. (29)–(31) can be used to determine the enhancement factor F for microchannel flow boiling. The two-phase thermophysical properties in the model can be estimated as the arithmetic mean of those of the liquid and vapor phases weighted by quality x:

$$\psi_{\text{tp}} = x\psi_v + (1-x)\psi_f \tag{32}$$

in which ψ is any thermophysical property. In the low-quality region, the differences in properties between single- and two-phase flows can be neglected as a first-order approximation. Under this approximation, the two-phase Reynolds number Re_{tp} can be derived from Eq. (18) as

$$\text{Re}_{\text{tp}} = \text{Re}_f F^3 \tag{33}$$

Suppression Factor S. The suppression factor S is usually obtained from regression analysis once the enhancement factor F is known [20]. Although this approach will also be used here, it is first desired to develop an analytical model for the suppression factor S that is independent of particular experimental data sets. Chen [20] pointed out that nucleate boiling during convective flow is governed by an effective superheat that is less than the wall superheat, which gives rise to a suppression of nucleate boiling heat transfer. Bennett et al. [50] proposed a theoretical approach to estimate the effective superheat for flow boiling in various types of boiling geometries. In the following, this approach will be modified to incorporate specific features of microchannel flow boiling.

It is postulated in this work that the fluid temperature varies linearly in the vicinity of the channel wall and is given by

$$T_f(y) = T_w + Ay \tag{34}$$

Considering the boundary condition $-k_f \partial T_f/\partial y|_{y=0} = \text{h}_{\text{conv}}(T_w - T_b)$, the temperature profile becomes

$$T_f(y) = T_w - \frac{h_{\text{conv}}}{k_f}(T_w - T_b)y \tag{35}$$

It is further assumed that the effective superheat within a distance y_0 from the wall, given by the following expression, is the driving force that governs nucleate boiling heat transfer:

Table 4 Values of the constant *C* in Eq. (30) [51]

Liquid	Vapor	Re_f	Re_g	Abbr.	C
Turbulent	Turbulent	>2000	>2000	tt	20
Viscous	Turbulent	<1000	>2000	vt	12
Turbulent	Viscous	>2000	<1000	tv	10
Viscous	Viscous	<1000	<1000	vv	5

$$\Delta T_s|_{y_0} = \frac{1}{y_0}\int_0^{y_0} [T_f(y) - T_b]dy \tag{36}$$

The suppression factor is then defined as the ratio of effective superheat $\Delta T_s|_{y_0}$ to the wall superheat $\Delta T_s(=T_w - T_b)$,

$$S = \frac{\Delta T_s|_{y_0}}{\Delta T_s} = 1 - \frac{h_{\text{conv}} y_0}{2k_f} \tag{37}$$

in which the two-phase convection heat transfer coefficient h_{conv} is obtained from Eq. (14).

The only unknown in Eq. (37), y_0, the thickness of the effective nucleate boiling region, can be approximated as the departure size of the bubble. In flow boiling, the departure size is determined by a balance of the forces acting on the vapor bubble. Due to the small bubble size in microchannel flows, surface tension and shear are the dominant forces (over inertia and buoyancy forces). According to Levy [52], the surface tension force F_s and shear force F_f are given by

$$F_s = C_s r_b \sigma \tag{38}$$

$$F_f = C_F \frac{\tau_w}{D_h} r_b^3 \tag{39}$$

Therefore, the bubble departure radius can be solved from a force balance, $F_s = F_f$, which yields

$$r_b = \sqrt{\frac{C_s \sigma}{C_F(\tau_w / D_h)}} \tag{40}$$

The thickness of the effective nucleate boiling region is then estimated as

$$y_0 = C\left(\frac{\sigma D_h}{\tau_w}\right)^{1/2} \tag{41}$$

where the empirical constant C is taken to be 0.35 in the present model. Compared to other values used in the literature [50,52], this value predicts a more reasonable bubble departure radius for water flow in microchannels [53]. The wall shear stress τ_w can be calculated from

$$\tau_w = 2f\frac{G^2}{\rho_f}$$

and

$$f = 96/\text{Re}_f(1 - 1.3553/\alpha + 1.9467/\alpha^2 - 1.7012/\alpha^3 + 0.9564/\alpha^4 - 0.2537/\alpha^5)$$

Further, the nucleate boiling coefficient in Eq. (11) is evaluated according to Gorenflo [54]:

$$h_{\text{nb}} = h_0 F_{\text{PF}} \left(\frac{q''}{q''_0}\right)^n \left(\frac{R_p}{R_{p0}}\right)^{0.133} \tag{42}$$

where the pressure correction factor F_{PF} for water is

$$F_{\text{PF}} = 1.73 p_r^{\,0.27} + \left(6.1 + \frac{0.68}{1 - p_r}\right) p_r^2$$

and p_r is the reduced pressure. The exponent n for the heat flux term is $n = 0.9 - 0.3 p_r^{\,0.15}$, and the reference values are $p_{r0} = 0.1$, $q''_0 = 20{,}000\ \text{W/m}^2$, $R_{p0} = 0.4\ \mu\text{m}$, and $h_0 = 5600\ \text{W/m}^2\,\text{K}$ [54]. The measured surface roughness at the bottom of the channel is approximately 1.5 μm, and the sidewalls are expected to be smoother, because of the method of fabrication. A value of 1 μm is sufficiently accurate for use in Eq. (42).

The suppression factor can also be derived through a regression analysis, as stated earlier. In this approach, S is correlated with the two-phase Reynolds number Re_{tp} as

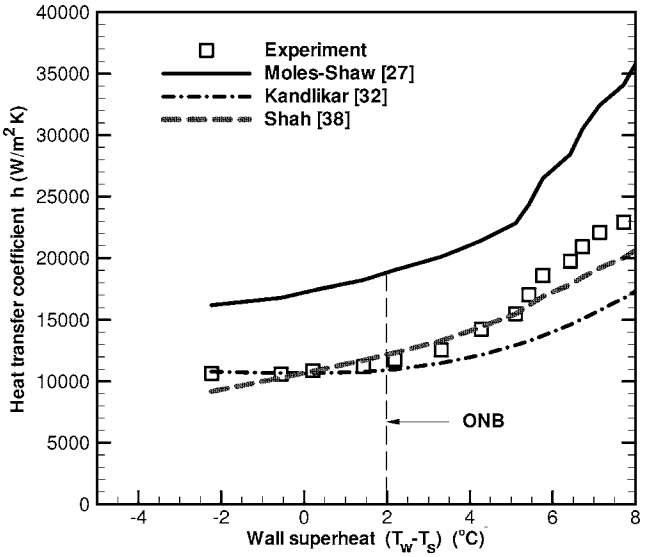

Fig. 8 Subcooled boiling heat transfer coefficient, case I-13 (G=921 kg/m² s, $T_{f,\text{in}}$=78.3 °C)

$$S = \frac{h_{\text{tp,exp}} - F h_{\text{sp}}}{h_{\text{nb}}} \propto \text{func}(\text{Re}_{\text{tp}}) \tag{43}$$

In Eq. (43), $h_{\text{tp,expt}}$ is the measured boiling heat transfer coefficient and h_{nb} is a selected correlation for the nucleate boiling heat transfer coefficient. Using this approach and the experimental data obtained in the present work, a new empirical correlation for suppression factor S is proposed for saturated flow boiling in microchannels:

$$S = \exp[36.57 - 55746/(\text{Re}_f F^3) - 3.4 \ln(\text{Re}_f F^3)] \tag{44}$$

5 Model Validation

5.1 Subcooled Boiling Regime. In the subcooled boiling regime, Eq. (8) reduces to

$$\bar{h} = [h_{\text{sp}} L_{\text{sp}} + h_{\text{sub}}(L - L_{\text{sp}})]/L \tag{45}$$

Figure 8 shows a comparison of the measured heat transfer coefficient, as defined in Eq. (6), with predictions using h_{sub} from various subcooled boiling correlations. In the regime following the occurrence of ONB, it is seen that the Shah correlation for subcooled boiling [38] offers very good predictions of the experimental data, while those of Moles–Shaw [27] and Kandlikar [32] overpredict and underpredict the heat transfer coefficient, respectively. It should be noted that the parameter ψ_0 used in Eq. (10) was originally developed for turbulent flow conditions, which is somewhat inconsistent with the laminar nature of microchannel flows. However, the Shah correlation is still recommended due to its agreement with the measured experimental data.

5.2 Saturated Boiling Regime. Figure 9 shows the predicted enhancement factor F calculated from Eq. (29) over the range of experimental conditions of the present work. The enhancement factor increases monotonically with the reciprocal of the Martinelli parameter, $1/X_{\text{vv}}$, which is proportional to the thermodynamic equilibrium quality. This suggests that the two-phase convective heat transfer is gradually augmented as more liquid is vaporized. Physically, the enhancement process may take place through different mechanisms. During the initial stage of boiling, two-phase flow usually appears in discrete bubbly form without significant interaction of adjacent nucleate bubbles. Individual bubble behavior, such as bubble departure and subsequent sliding on the channel surface [53], contributes in enhancement of the

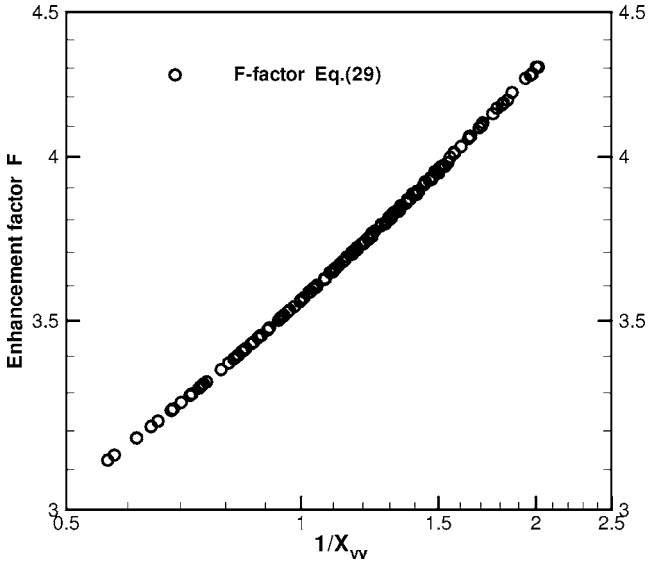

Fig. 9 Convective enhancement factor *F* as a function of laminar Martinelli parameter

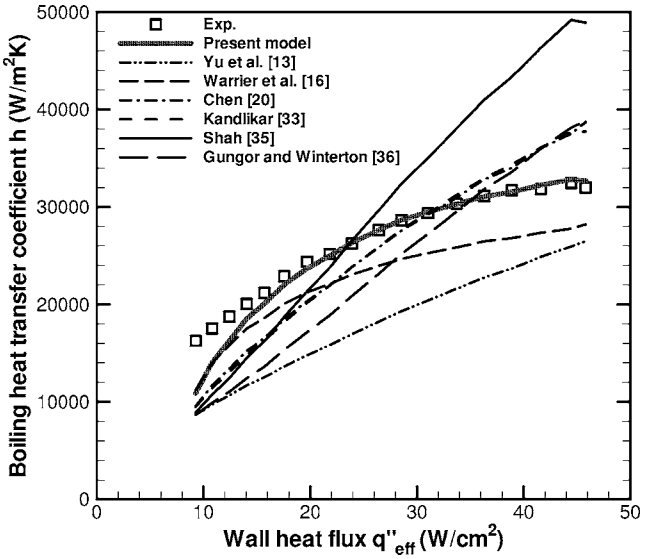

Fig. 11 Saturated boiling heat transfer coefficient, case II-2 (G=221 kg/m² s, $T_{f,in}$=91.7°C)

convective heat transfer by agitating the liquid in the thermal boundary layer. At higher qualities, the microchannel cross section is mostly occupied by the vapor phase due to the dramatic difference in the liquid and vapor densities. The liquid phase is then confined to a small portion of the microchannel cross section, either in a thin film around the channel periphery in annular flows or in short liquid slugs in slug flows. To ensure mass conservation, the effective velocity of the liquid phase is greater than the nominal value calculated by averaging over the entire cross section. In the proposed model, this effect is represented by the two-phase Reynolds number Re_{tp} defined in Eq. (33).

Figure 10 shows the predicted suppression factor S calculated from Eq. (44) using the regression analysis, which illustrates the decreasing trend of the suppression factor S as the two-phase Reynolds number Re_{tp} increases. This is caused by the intensified forced convection at high Re_{tp} that effectively reduces the superheat in the near-wall region. Alternatively, the suppression factor S may also be obtained analytically using Eq. (37).

Predictions of the boiling heat transfer coefficient from three widely cited saturated boiling models for conventional-sized channels [20,33,35], as well as from the correlation developed in the present work using the regression analysis result for S factor, are compared in Fig. 11 against the experimental measurements. Also shown are predictions from three correlation models for mini- and microchannel flows from the literature [13,16,36]. It is clear that the proposed correlation achieves the best agreement in the range of heat flux considered (for case II-2 shown in the figure), while most of the other models underpredict the experimental data at low heat flux and some [20,35,36] tend to overpredict the boiling heat transfer coefficient at high heat flux.

The validity of the proposed analytical model is further examined by comparing predictions for all the test cases in the experiments listed in Tables 2 and 3, as shown in Fig. 12. The agreement over the majority of the experiments is within ±35%. Model predictions using the suppression factor S from the regression analy-

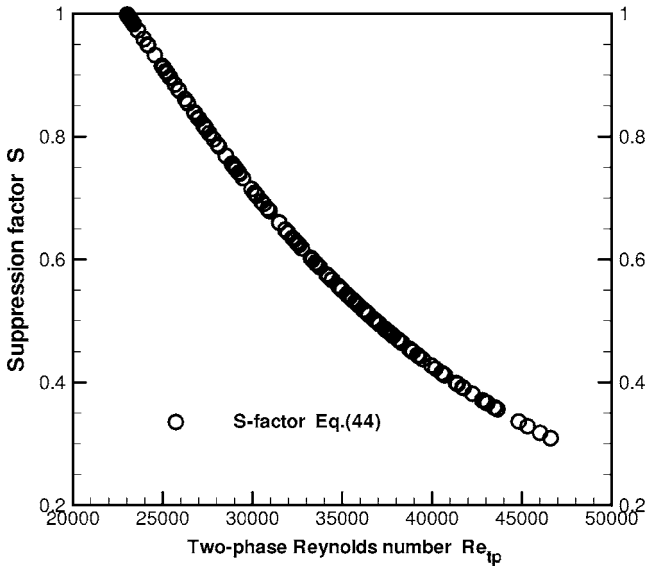

Fig. 10 Suppression factor *S* as a function of two-phase Reynolds number

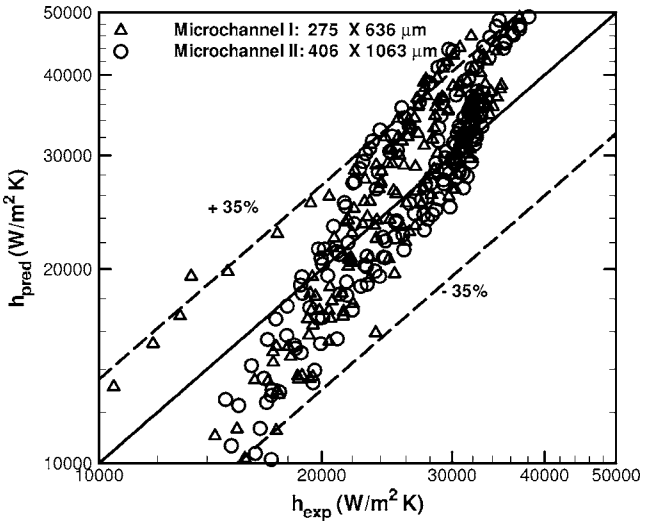

Fig. 12 Comparison of measured boiling heat transfer coefficients with those predicted with *S* factor obtained from analytical approach (Eq. (37)) (G=221–1283 kg/m² s, $T_{f,in}$ =66.6–95.4°C)

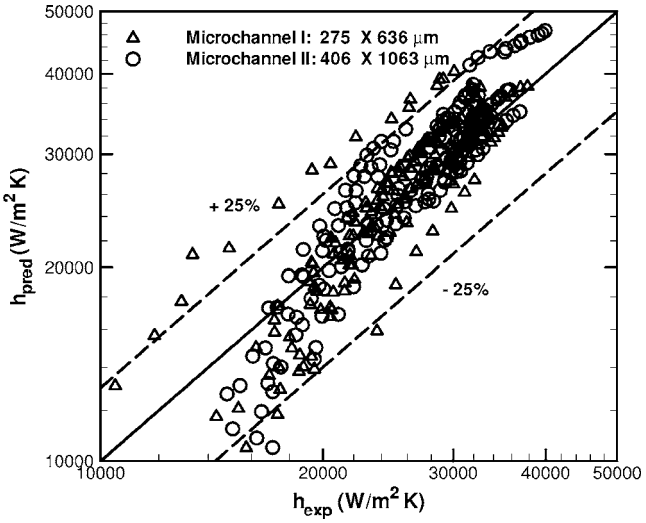

Fig. 13 Comparison of measured boiling heat transfer coefficients with those predicted with *S* factor obtained from regression analysis (Eq. (44)) (G=221–1283 kg/m^2 s, $T_{f,in}$ =66.6–95.4 °C)

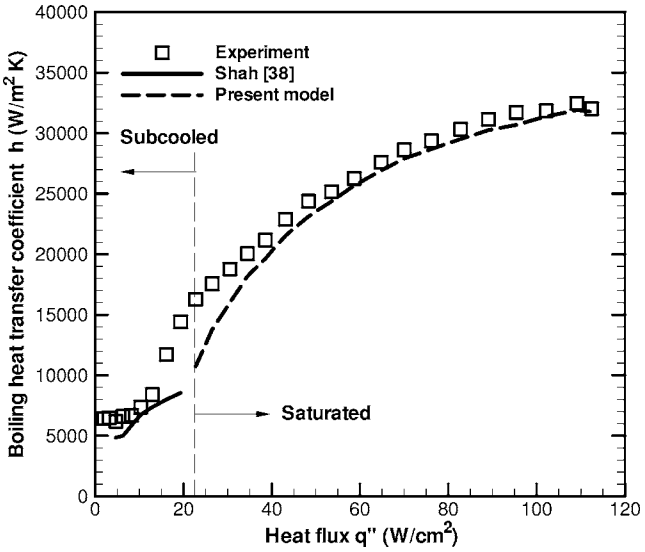

Fig. 14 Boiling heat transfer coefficient over subcooled and saturated regimes, case II-2

Table 5 Comparison with experiments of predictions from the present model (with *S* obtained both from analysis and regression) and other models in the literature

Model	Present (analytical)	Present (regression analysis)	Yu et al. [13]	Warrier et al. [16]	Chen [20]	Kandlikar [33]	Shah [35]	Gungor and Winterton [36]
MAE[a] (%)	16.7	10.9	32.0	14.1	22.7	20.5	34.6	25.7

[a](Mean absolute error is defined as $(1/N)\Sigma|h_{expt}-h_{pred}|/h_{expt}$)

sis approach (Eq. (37)) are plotted in Fig. 13, which shows better agreement with the experiments, within ±25%. The mean absolute errors (MAEs) associated with all models are calculated and listed in Table 5. The agreement of the proposed analytical model is significantly better than for predictions from almost any of the correlations in the literature for the present experimental data set, except for an empirical model in Ref. [16]. Considering the fact that there is still a systematic tendency to underpredict the heat transfer coefficient at the low range and overpredict it at the high range, more accurate predictions are being sought from detailed flow-pattern-based models.

5.3 Suggested Correlations. Based on the observations from the present study, the Shah correlation [38] is recommended for prediction of the boiling heat transfer coefficient in microchannels in the subcooled boiling regime, while the new correlations developed in the present work, Eq. (29) for enhancement factor F and Eq. (37) and (44) for suppression factor S, are recommended for the saturated boiling regime; this recommendation is illustrated for one representative case in Fig. 14.

6 Conclusions

Flow boiling of water in microchannels is experimentally investigated. The fluid and microchannel wall temperatures and the pressure drop across the microchannel were measured. The boiling heat transfer coefficients for subcooled and saturated boiling regimes were determined. Heat transfer correlations in the literature were assessed critically for applicability to microchannels. A new correlation suitable for the saturated boiling regime is developed. Suitable correlations to be used in the design of microchannel heat sinks in subcooled and saturated boiling at low qualities are suggested.

Key findings from this work are summarized as follows.

(1) The fluid inlet conditions, i.e., degree of subcooling and velocity, affect the onset of nucleate boiling, but have little impact on the boiling curve once the ONB has occurred.
(2) A critical review of conventional correlations in the literature suggests that the superposition-type heat transfer correlations are superior to the extrapolation-type in predicting the flow boiling heat transfer coefficient.
(3) The Shah correlation [38] provides satisfactory prediction of heat transfer coefficient in the subcooled boiling regime.
(4) A new heat transfer correlation is developed to predict the saturated boiling data, based on the model of Chen and co-workers [20,50]. Good agreement with the present experimental measurements indicates that this correlation is suitable for the design of two-phase microchannel heat sinks. Comparison with a larger database in the future is recommended.

Acknowledgment

The authors acknowledge the financial support from members of the Cooling Technologies Research Center, a National Science Foundation Industry/University Cooperative Research Center at Purdue University.

Nomenclature

A_b = area of microchannel heat sink, m^2
Bo = boiling number, Bo=q''/Gh_{fg}
Co = convection number, Co=$[(1-x)/x]^{0.8}(\rho_v/\rho_f)^{0.5}$
c_p = specific heat, kJ/kg °C
D_h = hydraulic diameter, μm
Fr = Froude number, Fr=$G^2/\rho_f^2 g D_h$
G = mass flux, kg/s m^2

h = heat transfer coefficient, $W/cm^2\,K$
h_{fg} = latent heat, J/kg
H_c = microchannel height, μm
i = enthalpy, J/kg
L = channel length, m
$\dot{m}$ = mass flow rate, kg/s
n = number of microchannels
p = pressure, Pa
Pr = Prandtl number
q'' = applied heat flux, W/cm^2
q''_w = effective heat flux, W/cm^2
Re = Reynolds number, $Re=GD_h\mu$
T = temperature, °C
u_0 = fluid inlet velocity, m/s
w_c = microchannel width, μm
w_w = microchannel fin thickness, μm
x = vapor quality
X = Martinelli parameter, $X^2=[(dp/dz)F]_f/[(dp/dz)F]_v$

Greek Symbols

α = microchannel aspect ratio
ϕ = two-phase multiplier
η = fin efficiency
ρ = density, kg/m^3
σ = surface tension, N/m

Subscripts

f = fluid
in = inlet
out = outlet
sat = saturated
sp = single phase
sub = subcooling
tp = two phase
v = vapor
w = wall

References

[1] Garimella, S. V., and Sobhan, C. B., 2003, "Transport in Microchannels—A Critical Review," Annu. Rev. Heat Transfer, **13**, pp. 1–50.
[2] Garimella, S. V., Singhal, V., and Liu, D., 2006, "On-Chip Thermal Management With Microchannel Heat Sinks and Integrated Micropumps," Proc. IEEE, **94**, pp. 1534–1548.
[3] Kandlikar, S. G., 2002, "Fundamental Issues Related to Flow Boiling in Minichannels and Microchannels," Exp. Therm. Fluid Sci., **26**, pp. 389–407.
[4] Bergles, A. E., Lienhard, V. J. H., Kendall, G. E., and Griffith, P., 2003, "Boiling and Evaporation in Small Diameter Channels," Heat Transfer Eng., **24**, pp. 18–40.
[5] Thome, J. R., 2004, "Boiling in Microchannels: A Review of Experiment and Theory," Int. J. Heat Fluid Flow, **25**, pp. 128–139.
[6] Lazarek, G. M., and Black, S. H., 1982, "Evaporative Heat Transfer, Pressure Drop and Critical Heat Flux in a Small Vertical Tube With R-113," Int. J. Heat Mass Transfer, **25**, pp. 945–960.
[7] Wambsganss, M. W., France, D. M., Jendrzejczyk, J. A., and Tran, T. N., 1993, "Boiling Heat Transfer in a Horizontal Small-Diameter Tube," J. Heat Transfer, **115**, pp. 963–972.
[8] Tran, T. N., Wambsganss, M. W., and France, D. M., 1996, "Small Circular- and Rectangular-Channel Boiling With Two Refrigerants," Int. J. Multiphase Flow, **5**, pp. 485–498.
[9] Kew, A. P., and Cornwell, K., 1997, "Correlations for the Prediction of Boiling Heat Transfer in Small-Diameter Channels," Appl. Therm. Eng., **17**, pp. 705–715.
[10] Yan, Y. Y., and Lin, T. F., 1998, "Evaporation Heat Transfer and Pressure of Refrigerant R-134a in A Small Pipe," Int. J. Heat Mass Transfer, **41**, pp. 4183–4194.
[11] Bao, Z. Y., Fletcher, D. F., and Haynes, B. S., 2000, "Flow Boiling Heat Transfer of Freon R11 and HCFC123 in Narrow Passages," Int. J. Heat Mass Transfer, **43**, pp. 3347–3358.
[12] Lee, H. J., and Lee, S. Y., 2001, "Heat Transfer Correlation for Boiling Flows in Small Rectangular Horizontal Channels With Low Aspect Ratios," Int. J. Multiphase Flow, **27**, pp. 2043–2062.
[13] Yu, W., France, D. M., Wambsganss, M. W., and Hull, J. R., 2002, "Two-Phase Pressure Drop, Boiling Heat Transfer, and Critical Heat Flux to Water in a Small-Diameter Horizontal Tube," Int. J. Multiphase Flow, **28**, pp. 927–941.
[14] Qu, W., and Mudawar, I., 2003, "Flow Boiling Heat Transfer in Two-Phase Microchannel Heat Sinks—I. Experimental Investigation and Assessment of Correlation Methods," Int. J. Heat Mass Transfer, **46**, pp. 2755–2771.
[15] Haynes, B. S., and Fletcher, D. F., 2003, "Subcooled Boiling Heat Transfer in Narrow Passages," Int. J. Heat Mass Transfer, **46**, pp. 3673–3682.
[16] Warrier, G. R., Dhir, V. K., and Momoda, L. A., 2002, "Heat Transfer and Pressure Drop in Narrow Rectangular Channels," Exp. Therm. Fluid Sci., **26**, pp. 53–64.
[17] Chen, T., and Garimella, S. V., 2007, "Flow Boiling Heat Transfer to a Dielectric Coolant in a Microchannel Heat Sink," IEEE Trans. Compon. Packag. Technol., **30**, pp. 24–31.
[18] Qu, W., and Mudawar, I., 2003, "Flow Boiling Heat Transfer in Two-Phase Microchannel Heat Sinks—Part II: Annular Two-Phase Flow Model," Int. J. Heat Mass Transfer, **46**, pp. 2773–2784.
[19] Thome, J. R., Dupont, V., and Jacobi, A. M., 2004, "Heat Transfer Model for Evaporation in Microchannels. Part I: Presentation of the Model," Int. J. Heat Mass Transfer, **47**, pp. 3375–3385.
[20] Chen, J. C., 1966, "Correlation for Boiling Heat Transfer to Saturated Fluids in Convective Flow," I&EC Process Des. Dev., **5**, pp. 322–329.
[21] Edelstein, S., Perez, A. J., and Chen, J. C., 1984, "Analytical Representation of Convective Boiling Functions," AIChE J., **30**, pp. 840–841.
[22] Steinke, M. E., and Kandlikar, S. G., 2004, "Control and Effect of Dissolved Air in Water During Flow Boiling in Microchannels," Int. J. Heat Mass Transfer, **47**, pp. 1925–1935.
[23] Collier, J. G., 1981, "Forced Convective Boiling," *Two-Phase Flow and Heat Transfer in the Power and Process Industries*, Hemisphere, Washington, DC, pp. 227–255.
[24] Taylor, J. R., 1997, *An Introduction to Error Analysis*, University Science Books, New York.
[25] Collier, J. G., and Thome, J. R., 1994, *Convective Boiling and Condensation*, Oxford University Press, Oxford, UK.
[26] Chen, T., and Garimella, S. V., 2006, "Measurements and High-Speed Visualizations of Flow Boiling of a Dielectric Fluid in a Silicon Microchannel Heat Sink," Int. J. Multiphase Flow, **32**, pp. 957–971.
[27] Moles, F. D., and Shaw, J. F. G., 1972, "Boiling Heat Transfer to Subcooled Liquids Under Conditions of Forced Convection," Trans. Inst. Chem. Eng., **50**, pp. 76–84.
[28] Webb, R. L., and Gupte, N. S., 1992, "A Critical Review of Correlations for Convective Vaporization in Tubes and Tube Banks," Heat Transfer Eng., **13**, pp. 58–81.
[29] Kutateladze, S. S., 1964, "Boiling Heat Transfer," Int. J. Heat Mass Transfer, **4**, pp. 31–45.
[30] Kandlikar, S. G., 1991, "Development of a Flow Boiling Map for Subcooled and Saturated Flow Boiling of Different Fluids Inside Circular Tubes," J. Heat Transfer, **113**, pp. 190–200.
[31] Papell, S. S., 1963, "Subcooled Boiling Heat Transfer Under Forced Convection in a Heated Tube," NASA-TN-D-1583.
[32] Kandlikar, S. G., 1997, "Heat Transfer Characteristics in Partial Boiling, Fully Developed Boiling, and Significant Void Flow Regions of Subcooled Flow Boiling," J. Heat Transfer, **102**, pp. 395–401.
[33] Kandlikar, S. G., 1990, "A General Correlation for Saturated Two-Phase Flow Boiling Heat Transfer Inside Horizontal and Vertical Tubes," J. Heat Transfer, **112**, pp. 219–228.
[34] Shah, M. M., 1976, "A New Correlation for Heat Transfer During Boiling Flow Through Pipes," ASHRAE Trans., **82**, pp. 66–86.
[35] Shah, M. M., 1982, "Chart Correlation for Saturated Boiling Heat Transfer: Equations and Further Study," ASHRAE Trans., **88**, pp. 185–196.
[36] Gungor, K. E., and Winterton, R. H. S., 1986, "A General Correlation for Flow Boiling in Tubes and Annuli," Int. J. Heat Mass Transfer, **29**, pp. 351–358.
[37] Liu, Z., and Winterton, R. H. S., 1991, "A General Correlation for Saturated and Subcooled Flow Boiling in Tubes and Annuli Based on a Nucleate Pool Boiling Equation," Int. J. Heat Mass Transfer, **34**, pp. 2759–2766.
[38] Shah, M. M., 1977, "A General Correlation for Heat Transfer During Subcooled Boiling in Pipes and Annuli," ASHRAE Trans., **83**, pp. 202–217.
[39] Steiner, D., and Taborek, J., 1992, "Flow Boiling Heat Transfer in Vertical Tubes Correlated by an Asymptotic Model," Heat Transfer Eng., **13**, pp. 43–68.
[40] Liu, D., Lee, P. S., and Garimella, S. V., 2005, "Prediction of the Onset of Nucleate Boiling in Microchannel Flow," Int. J. Heat Mass Transfer, **48**, pp. 5134–5149.
[41] Dittus, F. W., and Boelter, L. M. K., 1930, *Heat Transfer in Automobile Radiators of the Tubular Type*, University of California Publications of Engineering, University of California Press, Vol. 2, pp. 443–461.
[42] Sieder, E. N., and Tate, G. E., 1936, "Heat Transfer and Pressure Drop of Liquids in Tubes," Ind. Eng. Chem., **28**, pp. 1429–1436.
[43] Shah, R. K., and London, A. L., 1978, "Laminar Flow Forced Convection in Ducts," *Advances in Heat Transfer*.
[44] Lee, P. S., Garimella, S. V., and Liu, D., 2005, "Experimental Investigation of Heat Transfer in Microchannels," Int. J. Heat Mass Transfer, **48**, pp. 1688–1704.
[45] Rohsenow, W. M., 1952, "A Method of Correlating Heat Transfer Data for Surface Boiling of Liquids," Trans. ASME, **74**, pp. 969–976.
[46] Bennett, L., and Chen, J. C., 1980, "Forced Convective Boiling in Vertical Tubes for Saturated Components and Binary Mixtures," AIChE J., **26**, pp. 454–461.
[47] Forster, H. K., and Zuber, N., 1955, "Dynamics of Vapor Bubbles and Boiling Heat Transfer," AIChE J., **1**, pp. 531–535.

[48] Zhang, W., Hibiki, T., and Mishima, K., 2004, "Correlation for Flow Boiling Heat Transfer in Mini-Channels," Int. J. Heat Mass Transfer, **47**, pp. 5749–5763.
[49] Zhang, W., Hibiki, T., and Mishima, K., 2005, "Correlation for Flow Boiling Heat Transfer at Low Liquid Reynolds Number in Small Diameter Channels," J. Heat Transfer, **127**, pp. 1214–1221.
[50] Bennett, D. L., Davis, M. W., and Hertzler, B. L., 1980, "The Suppression of Saturated Nucleate Boiling by Forced Convective Flow," AIChE Symp. Ser., **199**, pp. 91–103.
[51] Delhaye, J. M., 1981, "Frictional Pressure Drops," *Two-Phase Flow and Heat Transfer in the Power and Process Industries*, Hemisphere, Washington, DC, pp. 98–150.
[52] Levy, S., 1967, "Forced Convection Subcooled Boiling Prediction of Vapor Volumetric Fraction," Int. J. Heat Mass Transfer, **10**, pp. 951–965.
[53] Liu, D., Lee, P. S., and Garimella, S. V., 2005, "Nucleate Boiling in Microchannels," J. Heat Transfer, **127**, p. 803.
[54] Gorenflo, D., 1993, *Pool Boiling: VDI-Heat Atlas*, VDI, Dusseldorf.